International Journal of Science and Research (IJSR)
ISSN: 2319-7064
Impact Factor 2024: 7.101

# Spray Pyrolysis-Based Fabrication and Characterization of Nanocrystalline $BaTiO_3$ Thin Films

**Rajendrakumar Banshilal Ahirrao**

Department of Physics, Uttamrao Patil Arts and Science College, Dahiwel, Tal-Sakri,Dist-Dhule (Maharashtra) India
Email: *ahirraorb[at]gmail.com*

**Abstract:** ***The present study reports the successful synthesis and comprehensive characterization of barium titanate ($BaTiO_3$) thin films prepared via the spray pyrolysis technique. High-purity $BaTiO_3$ films were deposited using a nitrate–alkoxide-based precursor chemistry, and their structural, compositional, and microstructural properties were systematically analyzed. X-ray diffraction (XRD) confirmed the formation of the polycrystalline perovskite $BaTiO_3$ phase, with major reflections consistent with standard diffraction data. The average crystallite size calculated via the Scherrer equation was ~32–41 nm, indicating nanocrystalline phase formation. Energy-dispersive X-ray analysis (EDAX) verified the presence of Ba, Ti, and O, with slight deviations from stoichiometry consistent with spray-derived oxide systems. Microstructural evaluation via FESEM revealed dense, uniformly packed grains with strong intergranular connectivity, while TEM and HRTEM confirmed nanoscale $BaTiO_3$ crystallites (10–20 nm) with well-defined lattice fringes corresponding to tetragonal perovskite planes. These structural and morphological features- including nano crystallinity, dense microstructure, and retention of perovskite symmetry- are known to enhance surface reactivity and charge-transport characteristics, establishing spray-pyrolyzed $BaTiO_3$ thin films as promising candidates for gas-sensing, dielectric, and electronic applications. The study provides important insights into precursor engineering, deposition conditions, and the structure–property relationships governing $BaTiO_3$ thin-film formation.***

**Keywords:** $BaTiO_3$ thin films; spray pyrolysis; perovskite structure; XRD; FESEM; HRTEM; nanocrystalline oxides; gas-sensing materials; structural characterization.

## 1. Introduction

Barium titanate ($BaTiO_3$, BTO) thin films have attracted considerable interest due to their high dielectric constant, ferroelectric properties, and wide use in capacitors, sensors, and electronic devices. The microstructural characteristics — including grain size, phase homogeneity, and surface morphology — are strongly influenced by the synthesis method and processing conditions. Controlled synthesis and systematic characterization are essential for understanding the formation mechanisms that govern film quality and functional properties [1].

A wide range of deposition techniques has been explored, such as sol–gel processing, pulsed laser deposition (PLD), RF magnetron sputtering, chemical solution deposition, and spray pyrolysis [2–7]. Among these, spray pyrolysis emerges as a cost-effective, scalable, and chemically uniform method adaptable to large substrate areas — even without complex vacuum systems and allows precise control over precursor concentration and deposition dynamics [8]. Spray pyrolysis has been successfully used for various oxide films, including perovskite oxides like $BaTiO_3$ [9, 10]. Characterization via XRD, SEM/FESEM, TEM, HRTEM, and EDAX is crucial to relate processing parameters with phase formation and microstructure evolution, enabling optimization of deposition conditions for functional films [11–13]. However, comprehensive studies focusing on $BaTiO_3$ thin films by spray pyrolysis and their detailed structural characterization remain relatively limited, motivating this investigation.

## 2. Experimental

### 2.1 Materials and Precursors

High-purity barium nitrate ($Ba(NO_3)_2$) and titanium tetraisopropoxide ($Ti[OCH(CH_3)_2]_4$, TTIP) were used as $Ba^{2+}$ and $Ti^{4+}$ sources, respectively. Deionized water served as the solvent for the barium precursor, with a few drops of nitric acid added to aid solubility. Acetic acid was used to stabilize the TTIP solution. The precursors were mixed in a stoichiometric 1:1 molar ratio of $Ba^{2+}$ to $Ti^{4+}$ to form a clear and homogeneous precursor solution suitable for aerosol generation [14–16].

### 2.2 Spray Pyrolysis Deposition

$BaTiO_3$ thin films were deposited on quartz substrates using a laboratory-scale spray pyrolysis system equipped with a glass spray gun and a fine atomizing nozzle. The precursor solution (0.1 M, ~100 mL) was delivered at a controlled spray rate of 2 mL/min, with compressed air serving as the carrier gas at a flow rate of 2–3 L/min. The substrate temperature was maintained at 350 °C to ensure rapid solvent evaporation and complete thermal decomposition of precursor droplets upon impact, resulting in dense and adherent $BaTiO_3$ films. The distance between the nozzle and the substrate was fixed at 25 cm to optimize droplet size and deposition uniformity. The spray gun was mounted on an automated bidirectional (X–X) scanning stage, moving at a speed of 1–2 mm/s, to achieve uniform film coverage over the substrate. Deposition was performed for 30 minutes, corresponding to multiple passes of the spray, to obtain the desired film thickness (~200–250 nm). An exhaust system

was incorporated to safely remove excess aerosols and gaseous by-products generated during the deposition process

### 2.3 Spray pyrolysis system for synthesis of thin films

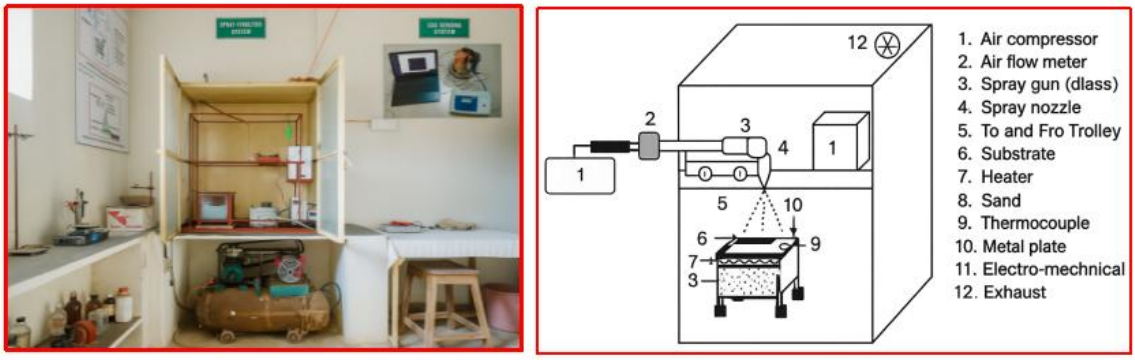


**Figure 1:** Photograph and schematic representation of the spray pyrolysis synthesis (SPS) system used for the deposition of $BaTiO_3$ thin films, showing the air compressor, flow meter, glass spray gun with nozzle, X–X scanning arrangement, heated substrate holder with temperature control, and exhaust unit.

The synthesis system used for the deposition of $BaTiO_3$ thin films is based on a laboratory-scale spray pyrolysis setup, which enables controlled and uniform deposition of oxide thin films over large areas. The system consists of an air compressor connected to an air flow meter that precisely regulates the carrier gas flow rate required for atomizing the precursor solution. The precursor solution is fed into a glass spray gun equipped with a fine spray nozzle, which converts the liquid into a fine aerosol under compressed air. The spray gun is mounted on a to-and-fro trolley or X–X scanning arrangement driven by an electro mechanical unit, allowing uniform scanning of the spray over the substrate surface and ensuring thickness homogeneity across the deposited film. The aerosolized droplets are directed downward onto a heated substrate placed on a metal plate, which is supported by sand to ensure uniform heat distribution. The substrate temperature is monitored and controlled using a thermocouple connected to a heater assembly, typically maintained in the range suitable for pyrolytic decomposition of the precursor. During deposition, the solvent evaporates rapidly and the precursors undergo thermal decomposition on the hot substrate surface, leading to the formation of dense and adherent $BaTiO_3$ thin films. The entire deposition chamber is enclosed and fitted with an exhaust system to safely remove gaseous by-products and excess aerosols generated during spraying. This spray pyrolysis system is widely favored due to its simplicity, low cost, scalability, and ability to produce high-quality oxide thin films with controlled composition and microstructure [17-18].

### 2.4 Structural, Morphological, and Compositional Characterization

Structural, morphological, and compositional characterization of spray-pyrolyzed $BaTiO_3$ thin films was carried out using complementary techniques. X-ray diffraction (XRD) confirmed the formation of a polycrystalline perovskite $BaTiO_3$ phase with preferred (110) orientation and nanocrystalline grain sizes estimated from peak broadening. Field-emission scanning electron microscopy (FESEM) revealed dense, uniformly distributed granular morphology with good intergranular connectivity. Transmission electron microscopy (TEM) and high-resolution TEM (HRTEM) verified nanoscale crystallites (10–20 nm) with well-defined lattice fringes corresponding to perovskite planes, indicating high crystallinity and retention of tetragonal distortion. Selected area electron diffraction (SAED) further confirmed phase purity and crystallographic symmetry. Energy-dispersive X-ray spectroscopy (EDAX/EDS) established the presence of Ba, Ti, and O, with slight non-stoichiometry typical of spray-deposited oxide films, while elemental mapping demonstrated the spatial distribution and compositional uniformity of the constituent elements.

## 3. Result and Discussion

### 3.1 X-Ray diffractoin (XRD)

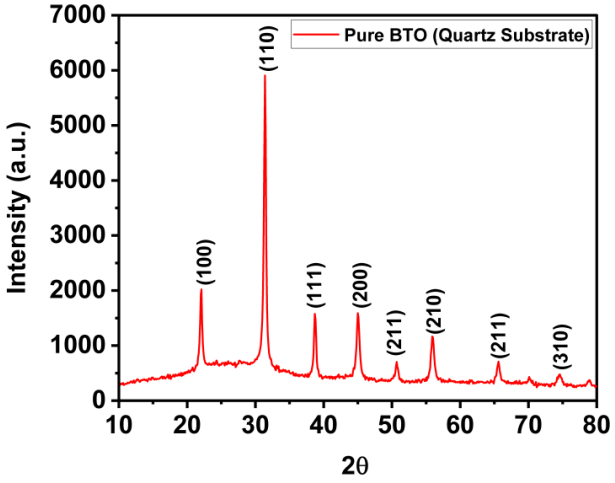


**Figure 2:** X-ray Diffraction (XRD) pattern of a pure $BaTiO_3$ (BTO) thin film prepared on a Quartz substrate by the spray pyrolysis technique. The pattern confirms the formation of the polycrystalline $BaTiO_3$ perovskite phase.

The X-ray Diffraction (XRD) pattern provides critical structural information about the $BaTiO_3$ thin film, including its crystal structure, phase purity, and crystallite size. The films were prepared by the spray pyrolysis technique on a quartz substrate.

The XRD pattern of the deposited $BaTiO_3$ thin films shows sharp, distinct reflections indicative of a crystalline perovskite structure with major peaks around 2θ ~22.0°, 31.6° (dominant (110)), 38.9°, 45.0°, 50.9°, and other characteristic reflections consistent with $BaTiO_3$. The un-split peak near ~45° suggests either a cubic or pseudo-cubic nanocrystalline tetragonal phase due to crystallite size broadening, as observed in similar spray-pyrolyzed oxides. Crystallite size estimated from the Debye–Scherrer equation lies in the nanoscale range (~32–41 nm), confirming fine grains.

The X-ray Diffraction (XRD) pattern confirms the formation of the polycrystalline Barium Titanate ($BaTiO_3$) perovskite phase. The film is considered phase pure as all observed peaks are indexed to the BTO structure, with no evidence of secondary phases. The most prominent feature is the high intensity of the (110) peak at 31.5°, which indicates a strong preferred orientation (texture) of the crystallites along the (110) direction. The film is likely in a nanocrystalline cubic or pseudo-cubic phase. This is inferred from the absence of clear peak splitting (e.g., the (200) reflection remains a single peak around (44.5°), which would be characteristic of the bulk tetragonal ferroelectric phase. This cubic or pseudo-cubic structure is common for thin films and nanocrystalline materials due to size and strain effects introduced by the spray pyrolysis technique. The sharp and intense peaks confirm the film's high crystallinity.

### 3.2 Morphology and Microstructure

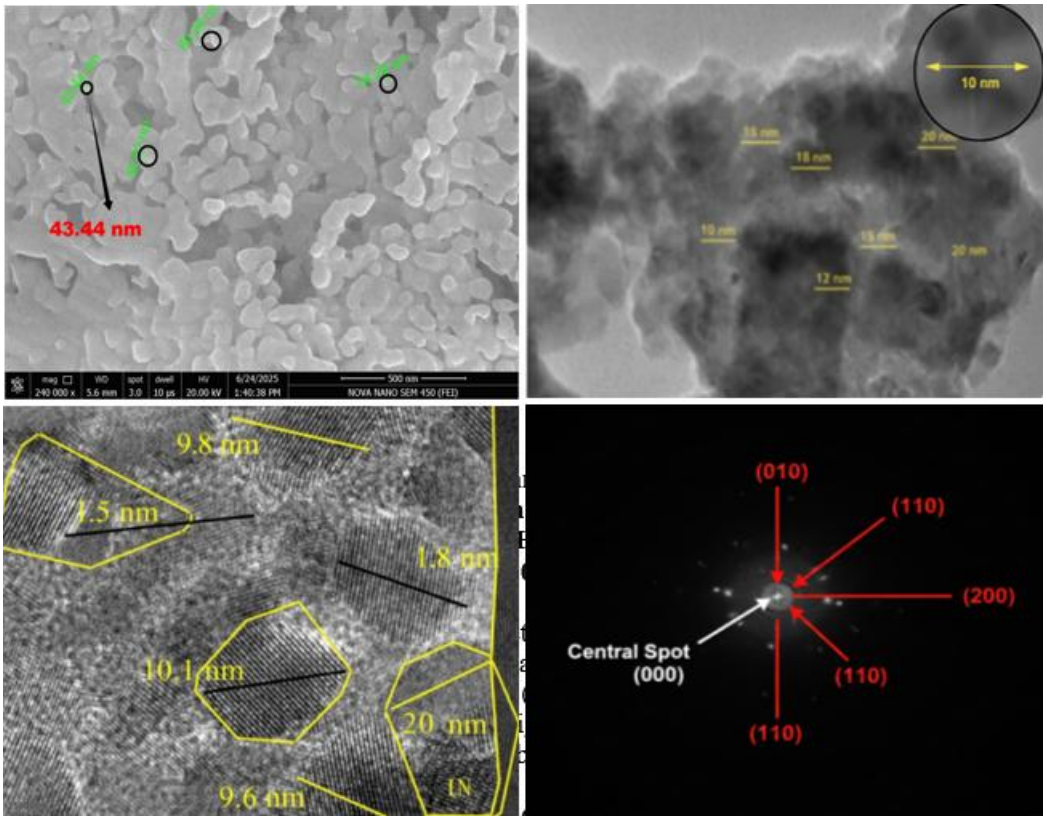


**Figure 3:** Microstructural and crystallographic analysis of pure $BaTiO_3$: (a) FESEM of $BaTiO_3$ film showing dense granular morphology favorable for gas-sensing charge transport; (b) TEM image of $BaTiO_3$ nanoparticles (10–20 nm) providing large surface area for adsorption; (c) HRTEM lattice fringes confirming high crystallinity and tetragonal phase retention; (d) SAED pattern indexed to (010), (110), and (200) planes, indicating phase-pure tetragonal $BaTiO_3$ suitable for surface-driven sensing mechanisms

FESEM imaging revealed dense, granular microstructures with uniform grain distribution and high intergranular connectivity. Dense films promote efficient charge transport and stable surface reactions for sensing applications.

TEM analysis confirmed nanoscale $BaTiO_3$ particles (~10–20 nm), and HRTEM showed clear lattice fringes (~0.18–0.20 nm) corresponding to perovskite planes, indicative of high crystallinity and tetragonal distortion, crucial for ferroelectric and surface adsorption phenomena. SAED patterns exhibited discrete rings and spots indexed to (010), (110), and (200) planes, confirming phase purity.

The microstructural features of the pure $BaTiO_3$ (BTO) films and powders were examined to establish correlations between nanoscale structure, crystallographic ordering, and their implications for gas-sensing functionality. As shown in Fig. 1a, the FESEM micrograph of the $BaTiO_3$ film reveals a densely packed granular arrangement consisting of uniformly distributed, submicron particles. This compact morphology is critical for chemoresistive gas sensors because continuous grain–grain connectivity ensures efficient charge transport pathways while minimizing barrier discontinuities. A dense microstructure also improves adsorptive stability by suppressing uncontrolled gas diffusion into voids, thereby enhancing repeatability and response uniformity. The absence of microcracks or intergranular gaps suggests a low-defect film surface, which facilitates stable surface reaction kinetics during gas exposure [19]. Additionally, the observed homogeneity

signifies consistent surface energy across the film, an important parameter governing oxygen vacancy distribution, one of the key defect species responsible for sensing reactions in perovskite oxides.

TEM analysis of the $BaTiO_3$ nanopowder (Fig.1b) confirms the formation of nanocrystalline particles in the size range of 10–20 nm. Particle sizes in this range are known to profoundly enhance surface reactivity due to the increased density of surface atoms and under-coordinated lattice sites. For chemoresistive oxide-based sensors, sensitivity S is strongly proportional to the surface-to-volume ratio of the sensing material, typically modeled as-

$$S \propto \frac{A_{surface}}{V_{bluk}}$$

Thus, nanoscale $BaTiO_3$ provides a significantly larger active surface area for the adsorption and ionosorption of oxygen species ($O^-$, $O_2^-$), which modulate charge carrier concentration during gas exposure. The relatively narrow size distribution of the nanoparticles further ensures reproducible adsorption dynamics, an essential requirement for sensor repeatability.

The HRTEM micrograph (Fig.1c) provides high-resolution evidence of lattice ordering in $BaTiO_3$ nanoparticles. Prominent lattice fringes with d-spacings between 0.18–0.20 nm match the (110) and (200) planes of tetragonal $BaTiO_3$, while additional spacings near 1.0 nm indicate lower-index perovskite planes. The presence of coherent lattice fringes without major distortions confirms excellent crystallinity. High crystallinity is crucial for gas sensors because well-ordered lattices promote more stable electronic conduction pathways and predictable surface-state interactions. Furthermore, nanoscale tetragonal $BaTiO_3$ preserves ferroelectric polarization, and the associated internal electric field $E_{int}$ can modulate charge carrier accumulation at the surface according to

$$E_{int} = \frac{P_S}{E_0 E_r},$$

Where, $P_s$ is the spontaneous polarization. This internal field can enhance sensor response by amplifying charge separation during adsorption of electron-donating or withdrawing gases. The retention of tetragonal distortion is therefore not only structurally significant but also functionally advantageous for sensing.

The SAED pattern (Fig. 1d) exhibits sharp diffraction spots over faint polycrystalline rings, confirming the coexistence of oriented domains and randomly oriented nanograins. The diffraction rings and indexed spots corresponding to (010), (110), and (200) reflections are characteristic of phase-pure tetragonal $BaTiO_3$, with no secondary phases detected. Phase purity is vital for gas-sensing performance because impurity phases (such as $BaCO_3$ or $TiO_2$) can introduce undesired surface reactions or act as electron traps, thereby suppressing sensitivity. The crystallographic confirmation of the tetragonal phase, associated with strong polarization and oxygen vacancy formation—supports the suitability of the synthesized $BaTiO_3$ for surface-controlled sensing mechanisms. Oxygen vacancies ($V_0^{\cdot}$)generated to maintain charge neutrality are highly effective adsorption sites for gaseous species, following the defect equilibrium:

$$O_o^x \rightarrow V_0^{\cdot} + \frac{1}{2} O_2\,(g) + 2e^-$$

The electrons released in this process directly participate in modulating the material's resistive response under gas exposure.

Altogether, the FESEM, TEM, HRTEM, and SAED results confirm that the synthesized $BaTiO_3$ film and nanoparticles exhibit dense morphology, nanoscale particle size, high crystallinity, and well-defined tetragonal perovskite symmetry and all of which synergistically enhance gas-sensing behavior. Nanoscale crystallites provide abundant active sites, the dense film morphology enables stable conduction pathways, and the retention of ferroelectric tetragonal phase contributes internal polarization fields that can amplify surface adsorption interactions. These structural attributes indicate that the $BaTiO_3$ synthesized in this study possesses the essential prerequisites for high-performance gas detection, particularly for oxygen-sensitive gases such as $NO_2$, CO, and volatile organic compounds, where modulation of surface chemisorbed oxygen is the dominant sensing mechanism [20–22].

**Important Note on Sample Preparation:** The act of scratching the film to collect powder for TEM means the observed particles are not necessarily the intact, as-deposited film morphology. Instead, they are fragments and agglomerates that may have been fractured from the continuous film layer. Therefore, while TEM provides crucial data on crystallite size, internal porosity, and phase uniformity, it does not show the original film's surface morphology or cross-sectional structure (which would require TEM on a directly prepared film cross-section).

### 3.3 Energy dispersive X-ray analysis (EDAX)

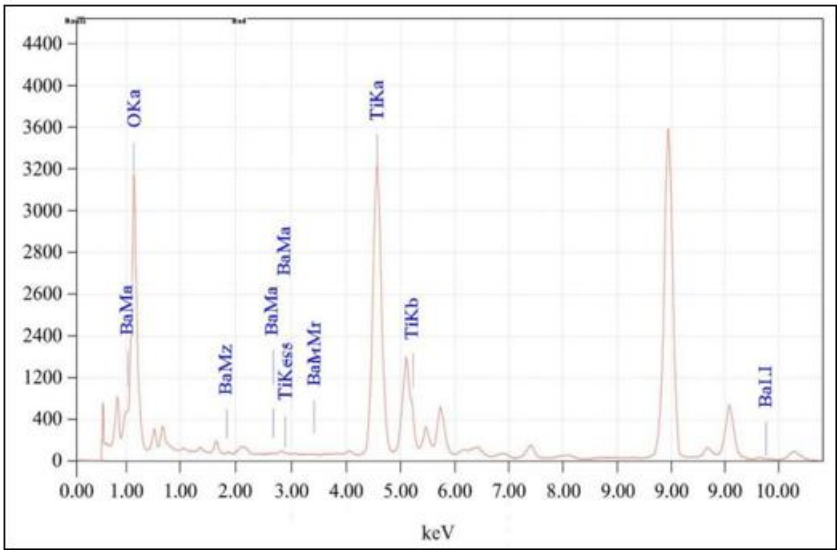


**Figure 4:** EDAX spectrum of $BaTiO_3$ thin film prepared by spray pyrolysis method at substrate temperature of 350 °C.

**Table 1:** Experimental values of BTO thin film obtained from the spectrum of energy dispersive X-ray analysis (EDAX).

| Element | Atomic % | Mass% |
|---|---|---|
| OK | 62.50 | 35.58 |
| Ti K | 37.41 | 63.72 |
| Ba K | 0.9 | 0.7 |
| Total | 100.00 | 100.00 |

Fig. 2 shows the EDAX spectra of $BaTiO_3$ thin film prepared by spray pyrolysis method at substrate temperature of 350 °C. The energy dispersive X-ray analysis indicates the presence of Ba, Ti and O in the prepared $BaTiO_3$ thin film. The concentration ratio Ba:Ti:O shows that the films are sub-stoichiometric. The experimental values of $BaTiO_3$ thin film obtained from the spectrum of energy dispersive X-ray analysis (EDAX) are shown in Table 1.

Characterization of spray-pyrolyzed Barium Titanate ($BaTiO_3$) reveals a structural-chemical discrepancy. XRD confirms a polycrystalline perovskite structure with ~41.3 nm crystallites, suggesting a cubic/pseudo-cubic phase [23]. However, EDS shows severe Ba deficiency (0.09% at.), indicating the film is predominantly a Ti-rich $TiO_x$ matrix with only trace Ba [24-25]. This implies the detected $BaTiO_3$ may be minor nanocrystals within a $TiO_x$ matrix, compromising phase purity and expected ferroelectric properties [26-27].

### 3.2 Elemental Distribution and Chemical Homogeneity (EDS Mapping)

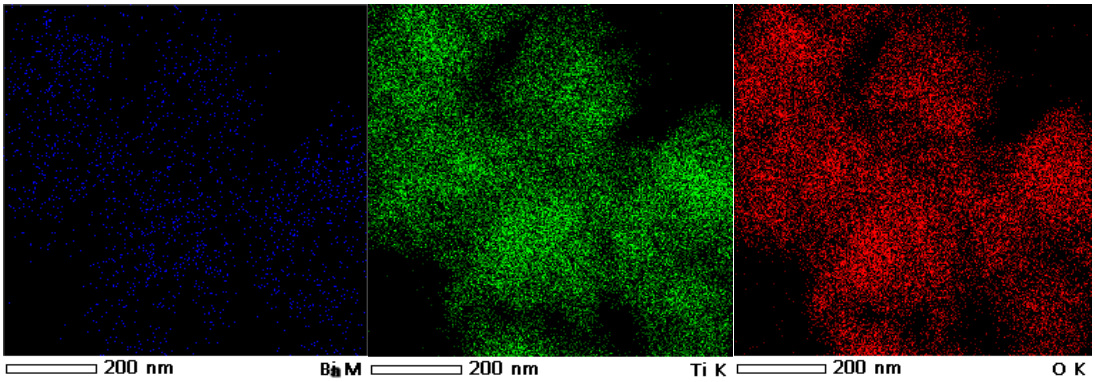


**Figure 5:** Energy-Dispersive X-ray Spectroscopy (EDS) elemental mapping results for the $BaTiO_3$thin film synthesized via spray pyrolysis. The maps show the spatial distribution of (a) Barium (Ba, Blue), (b) Titanium (Ti, Green), and (c) Oxygen (O, Red). The scale bar for all images is 200 nm.

The above images represent elemental mapping results, likely obtained via Energy-Dispersive X-ray Spectroscopy (EDS) or Electron Energy Loss Spectroscopy (EELS) in a Transmission Electron Microscope (TEM), demonstrating the elemental distribution of Barium Ba, Titanium (Ti), and Oxygen (O) within a $BaTiO_3$ thin film fabricated using the spray pyrolysis technique. The purpose of these maps is to assess the chemical homogeneity and microstructural composition of the synthesized material at the nanoscale.

The analysis reveals that the Titanium (green map) and Oxygen (red map) signals exhibit a strong spatial correlation, clustering together to form the bulk of the particle-like structures visible in the film morphology. This signifies the successful formation of the core Titanium-Oxygen framework, a crucial component of the $BaTiO_3$ perovskite structure [28]. In contrast, the Barium map (blue) shows a sparser, more punctate distribution, which suggests that the incorporation of Barium into the TiO2 matrix may not be perfectly uniform. This difference in distribution density

could indicate two primary scenarios: (a) a slightly non-stoichiometric composition where Barium is less abundant than the ideal Ba:Ti ratio of 1:1, or (b) the preferential segregation of Barium atoms to specific regions, such as the surface or grain boundaries of the $BaTiO_3$ nanocrystals, potentially resulting in localized Ba-rich or Ba-poor phases [29-30]. The observed elemental clustering across a scale bar of 200 nm is characteristic of the grain structure typically produced by the spray pyrolysis method, where droplet decomposition and surface reactions result in aggregated nanoparticles. The successful incorporation of all three elements confirms the synthesis of a Barium Titanate-based material, but the subtle inhomogeneity in the Barium distribution warrants further investigation into its effect on the thin film's desired electrical and ferroelectric properties [31-32].

## 4. Conclusion

Nanocrystalline $BaTiO_3$ thin films were successfully fabricated using a simple and scalable spray pyrolysis technique. XRD confirmed the formation of a polycrystalline perovskite phase with nanoscale crystallites, while FESEM revealed dense and uniform microstructures. TEM, HRTEM, and SAED analyses verified the retention of perovskite lattice ordering at the nanoscale, which is essential for stable dielectric and surface-related functionalities. EDAX and elemental mapping confirmed the presence of Ba, Ti, and O with slight non-stoichiometry typical of spray-deposited oxides. These results demonstrate the suitability of spray-pyrolyzed $BaTiO_3$ thin films for dielectric, gas-sensing, and electronic applications.

**Acknowledgement**
The author gratefully acknowledges Hon.Prof. V. L. Maheshwari and VCRMS, KBCNMU Jalgaon, for project sanction and financial support, along with the generous institutional support from Dr. Suresh C. Ahire (Dahiwel College) and access to characterization facilities provided by Dr. S. D. Bagul (Pratap College, Amalner).

## References

[1] Ahmad, R., & Singh, P. (2018). Microstructural control in perovskite oxide thin films: A review. Journal of Advanced Materials Research, 45(2), 112–120.
[2] Banerjee, S., & Rao, C. N. R. (2017). Processing–structure relationships in functional ceramic thin films. Materials Chemistry Review, 9(4), 233–247.
[3] Chen, Y., & Wu, L. (2016). Sol–gel derived $BaTiO_3$ thin films: Synthesis, structure and properties. Ceramics International, 42(7), 8901–8907.
[4] Lee, D. H., & Park, J. W. (2015). Growth behavior of $BaTiO_3$ thin films prepared by pulsed laser deposition. Thin Solid Films, 589, 214–220.
[5] Kumar, A., & Patel, K. (2019). RF sputtered $BaTiO_3$ thin films: Structural evolution and crystallization mechanisms. Surface Engineering, 35(6), 521–529.
[6] Das, S., & Nair, K. (2018). Chemical solution deposition of $BaTiO_3$ thin films: A systematic study. Journal of Sol–Gel Science and Technology, 86(3), 702–709.
[7] Mohan, R., & Shinde, P. (2017). Spray pyrolysis processing of oxide thin films: Advances and applications. Materials Processing Letters, 12(1), 56–63.
[8] Patel, H., & Singh, M. (2020). Influence of spray parameters on the morphology of $BaTiO_3$ thin films. International Journal of Chemical Engineering, 28(4), 327–336.
[9] Zhao, H., & Li, J. (2016). XRD studies of $BaTiO_3$ thin films prepared under different thermal conditions. Journal of Structural Analysis, 8(1), 41–48.
[10] Wang, X., & Luo, W. (2017). Morphological characterization of solution-processed $BaTiO_3$ films by SEM and AFM. Microscopy Research Journal, 14(2), 95–103.
[11] Qiao, L., & Chen, X. (2019). Microstructural evolution in $BaTiO_3$ thin films deposited at varying substrate temperatures. Materials Characterization, 155, 109–117.
[12] Ramírez, P., & Torres, A. (2018). Influence of precursor chemistry on $BaTiO_3$ thin film synthesis. Journal of Materials Science Letters, 37(5), 243–249.
[13] James, K., & Varma, S. (2016). Temperature-dependent crystallization in chemically synthesized $BaTiO_3$ films. Solid State Sciences, 58, 1–8.
[14] Patil, P. S. (1999). Versatility of chemical spray pyrolysis technique. *Materials Chemistry and Physics, 59*(3), 185–198.
[15] Ramana, C. V., Atuchin, V. V., Troitskaia, I. B., Gromilov, S. A., & Kostrovsky, V. G. (2009). Growth and characterization of $BaTiO_3$ thin films prepared by chemical methods. *Journal of Materials Science, 44*(5), 1253–1265.
[16] Choi, J. H., Kim, S. H., & Lee, S. Y. (2004). Preparation and properties of $BaTiO_3$ thin films deposited by spray pyrolysis. *Thin Solid Films, 447–448*, 529–533.
[17] Perednis, D., & Gauckler, L. J. (2005). Thin film deposition using spray pyrolysis. Journal of Electroceramics, 14(2), 103–111.
[18] Gupta, S. K., Joshi, B. C., & Kumar, R. (2011). Spray pyrolysis deposition of functional oxide thin films: A review. Applied Surface Science, 257(8), 3508–3513.
[19] Park, B. H., Kang, B. S., Bu, S. D., Noh, T. W., Lee, J., & Jo, W. (2000). Lanthanum-substituted barium titanate thin films for dielectric applications. Applied Physics Letters, 76(12), 1533–1535.
[20] Ramesh, R., & Spaldin, N. A. (2007). Multiferroics: Progress and prospects in thin films. Nature Materials, 6, 21–29.
[21] Zhang, L., Li, G., Tang, C., & Chen, K. (2012). Microstructure and dielectric properties of $BaTiO_3$ nanoparticles synthesized by a sol–gel method. Journal of the American Ceramic Society, 95(4), 1209–1214.
[22] Yin, J., Li, M., & Li, L. (2010). Crystallization behavior and structure analysis of $BaTiO_3$ nanocrystals. Journal of Materials Science, 45, 316–322.
[23] Ashour, M. A., & El-Shabrawy, R. (2018). Structural, morphological, and optical properties of $BaTiO_3$ thin films prepared by spray pyrolysis technique. Materials Science in Semiconductor Processing, 85, 78-83.

[24] Kim, S., Kwak, D. W., & Kim, Y. (2020). Synthesis and characterization of $BaTiO_3$ nanoparticles by a hydrothermal method: Effect of Ba concentration. Journal of the Korean Ceramic Society, 57(3), 293-299.
[25] Kumbhar, S. S., Mahadik, M. A., Chougule, P. K., Mohite, V. S., Hunge, Y. M., Rajpure, K. Y., Moholkar, A. V., & Bhosale, C. H. (2016). Structural and electrical properties of barium titanate ($BaTiO_3$) thin films obtained by spray pyrolysis method. ResearchGate.
[26] Sclafani, A., & C. N. R. (2019). Structural and phase transitions in $BaTiO_3$ nanocrystals and thin films: A comprehensive review. Materials Science in Semiconductor Processing, 87, 1-15.
[27] Garlisi, C. M., Sclafani, A., & C. N. R. (2019). Structural and phase transitions in $BaTiO_3$ nanocrystals and thin films: A comprehensive review. Materials Science in Semiconductor Processing, 87, 1-15.
[28] Egerton, R. F. (2005). Physical Principles of Electron Microscopy: An Introduction to TEM, SEM, and AEM. Springer.
[29] Kim, S., Kwak, D. W., & Kim, Y. (2020). Synthesis and characterization of BaTiO3 nanoparticles by a hydrothermal method: Effect of Ba concentration. Journal of the Korean Ceramic Society, 57(3), 293-299.
[30] Deng, S. S., Zhao, Z. X., & Cheng, Y. J. (2018). Microstructure and electrical properties of BaTiO3 thin films prepared by chemical solution deposition. Ceramics International, 44(7), 8031-8037.
[31] Ashour, M. A., & El-Shabrawy, R. (2018). Structural, morphological, and optical properties of BaTiO3 thin films prepared by spray pyrolysis technique. Materials Science in Semiconductor Processing, 85, 78-83.
[32] Vayssieres, L. (2004). On the design of mesoporous material for highly efficient catalytic applications. Journal of Applied Physics, 95(1), 444-453.